Human p53 Phosphorylation Mimic, S392E, Increases Nonspecific DNA Affinity and Thermal Stability†

Nicole Magnasco Nichols and Kathleen Shive Matthews*

Department of Biochemistry and Cell Biology, Rice University, Houston, Texas 77005

Received August 29, 2001; Revised Manuscript Received October 26, 2001

ABSTRACT: DNA binding is crucial to the protective role of the tumor suppressor protein p53, a nuclear phosphoprotein and transcription factor. The mutant human p53 protein S392E is a phosphorylation mimic that has been previously demonstrated to represent an "activated" form of p53 in both in vivo and in vitro assays [Hupp and Lane (1995) *J. Biol. Chem. 270*, 18165; Hao et al. (1996) *J. Biol. Chem. 271*, 29380]. Herein, we describe an analysis of structural and functional differences between this mutant and the wild-type protein. Structurally, the S392E protein exhibits increased thermal stability compared to wild-type p53, as monitored by circular dichroism and conformational antibody Ab1620 reactivity. These structural effects include alterations to the core DNA binding domain, remote in sequence space from the site of mutation. Functionally, the S392E mutation does not increase p53 binding to its 20 bp consensus DNA sequence in the absence of nonspecific DNA additives. In contrast, affinity of S392E for a 20 bp nonspecific DNA sequence is enhanced. Embedding 20 bp consensus DNA in the context of longer DNA sequences does not substantially alter S392E affinity, whereas wild-type affinity for these DNAs decreases with increased proportion of nonspecific DNA. These differences may account for the S392E "activated" phenotype and illuminate the role of this modified p53 in vivo.

Human p53 is a 393-amino acid tumor suppressor protein that binds to specific double-stranded DNA (dsDNA) segments and acts as a transcription factor in response to DNA damage and cellular stress (*1*−*8*). The majority of p53 mutants isolated from human tumors produce proteins with abrogated dsDNA binding function, reflecting the importance of DNA binding for in vivo function of this protein (*9*−*14*). Posttranslational modifications of the p53 protein include phosphorylation, acetylation, and potentially even glycosylation in response to various cellular signals (reviewed in refs *15* and *16*). Phosphorylation of the penultimate residue serine 392 (or serine 389 in murine p53) by casein kinase II (CKII)[1] is a well-established p53 modification (*17*, *18*) and has been reported to increase sequence-specific DNA binding (*19*−*22*).

Site-specific alterations at this penultimate residue have indicated the functional importance of serine phosphorylation. Alanine substitution at the murine serine residue homologous to position 392 in human p53 yielded protein that did not suppress cell growth in a transformation assay, whereas aspartic acid substitution resulted in protein with only slightly diminished function as compared to the wild-type protein in both transformed and normal cell lines (*23*). Thus, abolishing the CKII site by alanine substitution prevented normal p53 function, but substitution of a negatively charged amino acid (aspartate) was sufficient to mimic phosphorylation and partially rescue function in the murine protein. Similarly, Hall and colleagues (*24*) have reported that the murine aspartate mutant was able to repress transcription of the SV40 promoter at nearly wild-type levels, whereas this capacity for the alanine mutant was diminished. Further, substitution of the murine CKII serine with glutamic acid, but not alanine, activated transcription in contact-inhibited, but not actively growing, NIH3T3 cells, whereas glutamate substitutions at six other phosphorylation sites had no effect (*19*). However, alanine or aspartate substitution for S392 in human p53 did not affect activation of transcription or suppression of cell growth (*25*). The basis for the differential behavior observed in vivo between murine and human p53 proteins with CKII serine substitution is not apparent.

In vitro studies of CKII phosphorylation have provided evidence that wild-type p53 binding to a 26 bp consensus DNA sequence is enhanced by this modification, although equilibrium dissociation constants were not measured (*26*). In fact, numerous modifications of the C-terminus of p53, including Ab421 binding and C-terminal deletion, have been reported to result in increased apparent activity, implicating the C-terminus as a negative regulator of specific DNA binding (*21*, *26*−*28*). However, these data belong to a subset of experiments conducted in cell extracts or the presence of excess nonspecific DNA whose presence is now known to alter specific DNA binding results (*29*, *30*). Given these discrepancies, a thorough in vitro investigation of a protein with a negatively charged side chain at the CKII site is essential to determine the effects of an "activating" mutation on the structure and function of p53.

† This work was supported by grants from the G. Harold and Leila Y. Mathers Foundation and the Robert A. Welch Foundation (C-576). N.M.N. was supported in part by an NIH Molecular Biophysics Training Grant (GM-08280). Spectroscopic facilities were provided by the Keck Center for Computational Biology and the Lucille P. Markey Charitable Trust.

* To whom correspondence should be addressed. Phone: 713-348-4871; fax: 713-348-6149; e-mail: ksm@rice.edu.

[1] Abbreviations: BSA, bovine serum albumin; CKII, casein kinase II; conDNA, p53 consensus DNA sequence; DTT, dithiothreitol; Pu, purine; Py, pyrimidine; p53RE, p53 response element.

10.1021/bi011736r CCC: $22.00 © 2002 American Chemical Society
Published on Web 11/29/2001

To provide an unmodified background against which a glutamate substitution could be assayed, the human S392E protein was purified from *Escherichia coli*. Strikingly, as compared to the wild-type protein, the mutant displays increased thermal stability, as monitored by circular dichroism, as well as increased reactivity to the conformational antibody Ab1620 at 42 °C. Enhanced thermal stability is also evident in the largely unaltered affinity for specific DNA as a function of temperature, resulting in a diminished change in heat capacity as compared to the wild-type protein. Despite these structural differences between the mutant and wild-type proteins, the "activated" form of p53 does not demonstrate increased affinity for the 20 base pair consensus DNA sequence at room temperature. However, the S392E protein exhibits the same affinity for 20, 40, and 60 base pair target DNAs containing the 20 base pair consensus DNA sequence, whereas wild-type protein demonstrates reduced affinity as the target length (and percentage of nonspecific DNA) is increased. The relative enhanced affinity of S392E for DNA targets that embed the consensus sequence in extended nonspecific sequences may derive from increased S392E affinity for nonspecific DNA.

MATERIALS AND METHODS

Plasmids and Cell Strains. The human p53 gene cloned into the pET15b expression plasmid and hybridoma cells expressing the monoclonal p53 antibody Ab421 were generous gifts from the laboratory of Dr. G. Lozano (M. D. Anderson Cancer Center, Houston, TX). The p53 gene was excised from pET15b and cloned into a pRSET plasmid using *Xba*I and *Bam*HI restriction enzyme sites. The pRSET vector contains an F1 origin, necessary for single-stranded mutagenesis. This insert contained the p53 gene as well as 491 base pairs of genomic sequence at the 3′ end of the gene, and the resulting construct was named pSET53. *E. coli* strain DH5α was used to prepare all double-stranded DNAs. *E. coli* BL21(DE3) cells, with or without the pLysS episome (Novagen), were used for expressing wild-type and mutant p53 proteins.

Mutagenesis and Protein Purification. Single-stranded mutagenesis (*31*) was performed on pSET53 to generate a glutamic acid substitution for the wild-type serine at position 392 (S392E), the penultimate amino acid. Full gene sequencing verified the mutation and the integrity of the remainder of the p53 gene. Proteins were expressed and purified as described previously (*30*) with a final elution from a phosphocellulose column approximately midway through a 0.2−0.5 M KPB [potassium phosphate buffer, pH 7.5, 5 mM DTT, 10% (v/v) glycerol and 5% (w/v) glucose] gradient. Fractions were confirmed to contain p53 by Western analysis with either monoclonal antibody Ab421 (*32*) or Ab240 (*33*). Protein purity (∼80−90% for each preparation) was assessed by SDS−PAGE analysis and confirmed by densitometry. Protein concentration was determined by Bio-Rad assay (*34*) and by absorbance at 280 nm using the Beer−Lambert Equation where the extinction coefficient was calculated from amino acid content. Because of significant protein loss upon concentration or dialysis, the purified protein samples were used in all assays as eluted from the column in ∼0.35 M KPB or diluted into a lower molarity potassium phosphate buffer as specified.

Determination of Assembly. A Beckman XL-A analytical ultracentrifuge was used in sedimentation velocity and equilibrium experiments. Two-channel sector cells were used for velocity experiments, and six-channel sector cells were used for equilibrium experiments. Experiments were conducted at 22 °C, and absorbance was monitored at 220 nm. Equilibrium experiments were conducted at three concentrations (1.1×10^{-6}, 9.0×10^{-7}, and 7.5×10^{-7} M_{tet}) and three speeds (7000, 9000, and 11000 rpm) to eliminate possible effects of either concentration or speed on the final analysis. The resulting data are best fit to a tetramer, but are complicated by the formation of higher order oligomers. S392E displays a slightly increased tendency to form higher ordered species, but no quantitative analysis was possible. Despite the complications due to larger complexes, the data cannot be well described by any model that includes monomeric or dimeric species, confirming that the majority of p53 protein is present as tetramers or higher order oligomers.

Circular Dichroism − Thermal Denaturation. Circular dichroism spectra were collected on an AVIV model 62A DS circular dichroism spectrometer equipped with Star 3.0 Stationary. 10-Camphorsulfonic acid was used as an internal standard. S392E protein was either at 7.2×10^{-7} or 1.4×10^{-6} M_{tet}, in either ∼0.35 M KPB or buffer D [∼0.2 M potassium phosphate buffer, pH 7.5, 2.5 mM DTT, 5% (v/v) glycerol, and 2.5% (w/v) glucose]. Both conditions yielded similar results. For spectra shown, wild-type p53 was at a protein concentration of 8.0×10^{-7} M_{tet}, in the buffer in which the protein was purified, ∼0.35 M KPB. Spectra were collected in 0.5 nm increments from 255 to 200 nm with an 8 s/point averaging time in a quartz cuvette with a 0.2 cm path length. The slit width was regulated throughout the scan. Baseline buffer spectra were subtracted from sample spectra prior to averaging the points along each temperature curve. Data points were converted to $\Delta\epsilon$ using the Beer−Lambert equation,

$$\Delta\epsilon = \epsilon(L) - \epsilon(R) = \frac{\Delta A}{cl} \quad (1)$$

where c is the concentration of p53 expressed in M tetramer, l is the cuvette path length in cm, and ΔA is the measured CD signal. The spectra were then smoothed (bounce, $n = 7$) and plotted in Igor Pro (Wavemetrics). Temperature was monitored at the sample compartment with a computer-controlled Peltier device. For each temperature, the sample was equilibrated in the cell holder for 3 min before full wavelength scans were collected. To ensure that protein concentrations were unchanged during the experiment and to monitor aggregation, absorbance was measured at 280 and 600 nm over the same temperature range. A slight increase in absorbance at 280 nm was observed, but no change was noted at 600 nm.

Spectra were collected from 0 to 100 °C in 10 degree steps. The results from multiple independent runs were averaged. Similar data were obtained on at least three different protein preparations. Data points at 218 and 210 nm were expressed as a fraction of the initial signal (at 0 °C) as a monitor of β-sheet and α-helical content, respectively. The data were fit to a modified Michaelis−Menten equation to estimate the midpoint of irreversible unfolding. CD spectra of p53 were

also collected as a function of time (up to 120 min) to verify that equilibrium was reached at each temperature in the range investigated (data not shown).

Conformational Antibody Experiments. Purified wild-type and S392E p53 proteins were diluted to a final concentration of 3.0×10^{-7} M_{tet} in 0.3 M KPB with 0.1 mg/mL BSA. Samples were incubated at 0, 5, 16, 22, 37, 42, 50, or 65 °C for 30 min before rapid filtration at room temperature onto a nitrocellulose filter presoaked in potassium phosphate buffer. Temperature measurements for samples containing buffer in the absence of protein were used to establish that no significant temperature change occurred during filtration. The nitrocellulose filter was blocked with 10% dry milk in PBST [phosphate buffered saline, pH 7.4, 0.05% (v/v) Tween 20] for 30 min and exposed to either Ab1620 (conformation dependent) or Ab421 (conformation independent) overnight at 4 °C. After thorough washing with PBST, the filter was incubated with a secondary antibody complexed to horseradish peroxidase for 1 h at room temperature followed by PBST washes. The use of an ECL kit (Amersham) and subsequent film exposure allowed visualization of the reaction. Reactivity was quantitated by a Molecular Dynamics Computing Densitometer equipped with ImageQuant software and normalized to the reactivity of the 0 °C sample for each experiment. Normalized data from independent runs were averaged and reported.

DNA Binding. A variation of the 96-well nitrocellulose filter assay first described by Wong and Lohman (*35*) was used to determine equilibrium dissociation constants for p53 binding to a 20 bp consensus sequence (conDNA), a 20 bp nonspecific sequence (NS2), and 40 bp (40DNA) and 60 bp (60DNA) sequences that contained the 20 bp consensus sequence. These measurements were made under nonstoichiometric conditions (i.e., DNA concentration well below K_d). All sequences reported (and their complements) were commercially synthesized (Great American Gene Co. or Sigma Genosys). The conDNA sequence and its complement are based on the p53 consensus DNA operator (Figure 1A), consisting of two repeats of the 10 base pair motif 5′-PuPuPuC(A/T)(T/A)GPyPyPy (*3*, *4*). DNA binding assays to determine nonspecific DNA binding by p53 employed a 20mer sequence and its complement, termed NS2 (Figure 1A). NS2 was designed to contain the identical base composition as conDNA while at the same time using as many of the least used residues as possible at each position. 40DNA and 60DNA were designed as longer double-stranded DNA targets containing the 20 bp conDNA sequence. 40DNA contains 10 base pairs of random sequence on both the 5′- and 3′-ends, and 60DNA contains 30 base pairs of nonspecific sequence at one end and 10 base pairs flanking the other end of the conDNA sequence (Figure 1B). Complementary DNAs were annealed to form blunt-end double-stranded targets and labeled at the 5′-ends using γ-[^{32}P]-ATP and polynucleotide kinase incubated at 37 °C for 1 h. Protein from 1.0×10^{-7} to 1.0×10^{-11} M_{tet} was incubated with 2×10^{-11} M DNA, a concentration well below the K_d for all protein−DNA interactions measured.

Buffer used to dilute the protein samples contained 0.1 mg/mL BSA to minimize aggregation and adherence of protein. The protein−DNA samples were incubated for 30 min at the temperature indicated (from 0 to 50 °C) in 0.05 M potassium phosphate buffer, pH 7.5, before rapid filtration

A

Consensus Analysis	5′	R	R	R	C	W	W	G	Y	Y	Y	3′
	A	40	20	55	0	53	15	0	0	0	12	A
	C	13	3	3	93	8	0	0	50	68	35	C
	G	23	70	40	0	8	3	100	0	0	3	G
	T	23	5	0	5	30	82	0	50	30	48	T

ConDNA:												
Left half site	5′	A	G	A	C	A	T	G	C	C	T	3′
Right half site	5′	A	G	A	C	A	T	G	C	C	T	3′
NS2:												
Left half site	5′	T	C	C	A	G	A	T	G	T	A	3′
Right half site	5′	C	C	C	A	A	A	C	G	T	G	3′

B

ConDNA **AGACATGCCTAGACATGCCT**

NS2 TCCAGATGTACCCAAACGTG

40DNA TGTTGTGTGG**AGACATGCCTAGACATGCCT**TTCACACAGG

60DNA TCCAGATGTACCCAAACGTGTGTTGTGTGG**AGACATGCCTAGACATGCCT**TTCACACAGG

FIGURE 1: Comparison of conDNA and NS2 to the p53 consensus site. (A) p53 consensus site was derived from numerous naturally occurring p53 response element sequences and determined to be comprised of two repeats of the half site 5′-RRRCWWGYYY, where R is any purine, Y is any pyrimidine, and W is A or T (underlined in each column) (*3*). Numbers indicate the percent representation for each nucleotide at each position in this sequence (*3*). ConDNA is two repeats of a sequence whose pattern matches the consensus site. NS2 was designed to match as many as possible of the least used base pairs per position, while at the same time maintaining an identical base composition to conDNA: 10 G−C and 10 A−T pairs. Only one strand of each double-stranded target sequence is depicted. (B) The sequence of 40DNA is comprised of the conDNA 20mer target with 10 base pairs of flanking nonspecific sequence. 60DNA is composed of 40DNA with the addition of the 20 base pair sequence of NS2. Complementary sequences were annealed to create blunt end double-stranded DNA targets for all DNA binding experiments.

through nitrocellulose paper (Schleicher & Schuell). The nitrocellulose filter was dried at 65 °C for 5 min and then exposed to a phosphorimaging plate at room temperature. A Fuji Phosphorimager was used to quantitate the pixels, and a value for a background point with no protein was subtracted from each corresponding condition with protein (Fuji MacBas Software).

Values from multiple sets of experiments were fit (Igor Pro) according to the following equation,

$$R = Y_{max}\frac{[p53]^n}{[p53]^n + K_d^n} \quad (2)$$

where R is the amount of bound complex at a specific protein concentration divided by the amount of bound complex at saturating protein, Y_{max} is a correction factor that allows for the R value at saturation to float, K_d is the apparent equilibrium dissociation constant, [p53] is the concentration of total p53 protein expressed in tetramer, and n is the Hill coefficient. Binding isotherm data are the compilation of multiple assays performed in duplicate. The value of n for wild-type−conDNA and S392E−conDNA did not vary significantly as a function of temperature, although Hill coefficients for nonspecific binding were lower for both proteins as compared to specific binding.

Protein activity assays were conducted both at room temperature and at 50 °C for the wild-type and S392E proteins by stoichiometric titrations with conDNA as described above, but with conDNA concentration above the K_d at 2×10^{-8} M and protein concentrations from 5.0×10^{-9} to 3.0×10^{-7} M_{tet} to reach saturation levels. Activity assays were conducted similarly for both proteins with 40DNA and 60DNA. Protein concentrations for each experi-

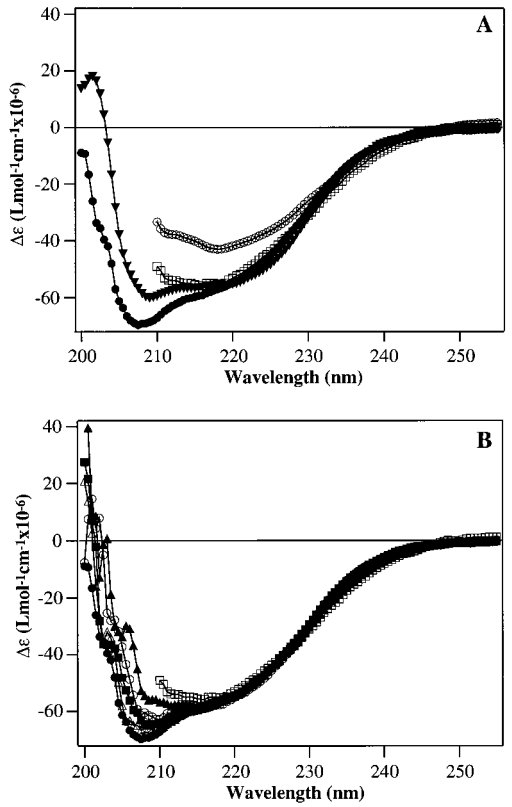

FIGURE 2: Circular dichroism spectra as a function of temperature. Spectra were collected from 0 to 100 °C using wild-type (WT) or S392E protein concentrations from 0.7 to 1.4 × 10^{-6} M tetramer in ~0.35 M KPB. Before plotting, spectra were corrected for baseline and smoothed (bounce, $n = 7$). (A) A comparison of spectra collected at both 0 and 100 °C for wild-type and S392E demonstrate significant thermal stability of the mutant protein as well as increased intensity at ~208 nm, a wavelength typically indicative of α-helical structure. (●) S392E, 0 °C, (□) S392E, 100 °C, (▼) WT p53, 0 °C, (⊕) WT, 100 °C. (B) CD spectra of S392E were collected as a function of temperature from 0 to 100 °C in 10 °C increments, and every other spectrum is depicted. Although intensity at ~208 nm varies as a function of temperature, CD signal at 218 nm remains largely unchanged. Symbols are as follows: (●) 0 °C, (△) 20 °C, (■) 40 °C, (○) 60 °C, (▲) 80 °C, (□) 100 °C.

ment to determine equilibrium dissociation constants were corrected to reflect the relative activity of the sample, which ranged from ~30−50% per preparation. DNA binding data collected as a function of temperature were analyzed using a van't Hoff plot fit to the equation modified from Ha et al. (*36*) as reported previously (*30*).

RESULTS

Thermal Denaturation of Mutant p53. S392E was purified from *E. coli* using methods similar to those for wild-type p53. The purified protein was examined by analytical ultracentrifugation, and the assembly state was primarily tetrameric with no evidence of monomeric or dimeric species (data not shown). However, S392E displayed a slightly greater tendency to form aggregates of higher order than tetramer in comparison to behavior for the wild-type protein.

The secondary structure of S392E was examined using circular dichroism spectroscopy to determine the effects of this "activating" mutation on the thermal stability of the protein. Similar to wild-type p53, contributions from both β-sheet (~218 nm) and α-helical (~208 nm) structure are

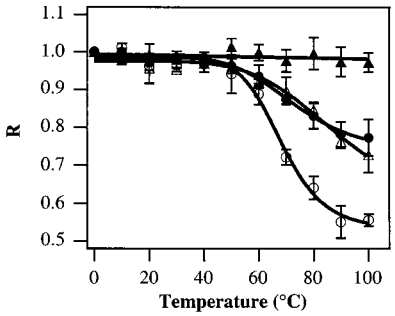

FIGURE 3: Comparison of thermal stability for wild-type and S392E proteins. The fraction of residual structure of S392E (triangles) and wild-type (circles) is shown as a function of temperature. The circular dichroism signal at 0 °C is defined as 1 for each experiment. Data are taken from two wavelengths to monitor α-helical (210 nm, open symbols) and β-sheet (218 nm, filled symbols) structure. Because thermal denaturation is not reversible, unfolding midpoints are estimated based on a modified Michaelis-Menton equation and can be used only for comparative purposes. Values for wild-type protein, as reported previously (*30*), are ~73 °C at 218 nm and ~68 °C at 210 nm. An unfolding midpoint for the helical structure within the mutant protein could be estimated from the data at 210 nm (~83 °C), whereas no unfolding was observed for the β-sheet structure at 218 nm.

evident at the lowest temperatures (Figure 2A). However, the intensity of the 208 nm minimum is increased as compared to wild-type p53, suggesting a greater contribution of α-helical structure in the mutant protein than seen for the wild-type structure. Whether increased α-helical structure occurs within the C-terminal region itself or other regions of the protein cannot be discerned. Whereas the wild-type protein loses signal characteristic of β-sheet structure (~218 nm) from 60 to 100 °C, the mutant displays no observable loss in this signal at any of the temperatures investigated (Figure 2B). Hour-long incubations of S392E and wild-type protein (*30*) were conducted at 90 °C to verify this result, and no signal change was observed under these conditions (data not shown).

Although analysis of the data for wild-type β-sheet structure at 218 nm indicates a midpoint of ~73 °C for the unfolding transition, a similar estimate is not possible with S392E since no decrease in signal at this wavelength occurs (Figure 3). As reported previously (*30*), the β-sheet structure can be ascribed to the core DNA binding domain of the protein, suggesting that this region is more stable in the mutant protein. To estimate the T_m for the α-helical unfolding transition, data points at 210 nm were examined as a function of temperature (Figure 3). The increased interference of DTT at wavelengths lower than 210 nm precluded examination at 208 nm, a standard wavelength monitored for α-helical structure. The midpoint of the 210 nm wild-type data occurs at ~68 °C. The midpoint of the S392E data is estimated to occur at ~83 °C; however, this value can be considered a minimum based on the absence of a plateau at elevated temperatures.

Conformational Antibody Reactivity of S392E. For wild-type p53, the loss of the Ab1620 epitope within the DNA binding core domain at temperatures >37 °C has been used to diagnose the presence of inactive protein, and positive reactivity has been used to indicate folded and active protein (*37*). However, we have shown recently that loss of reactivity occurs prior to loss of specific DNA binding for the bacterially produced wild-type protein (*30*), precluding direct

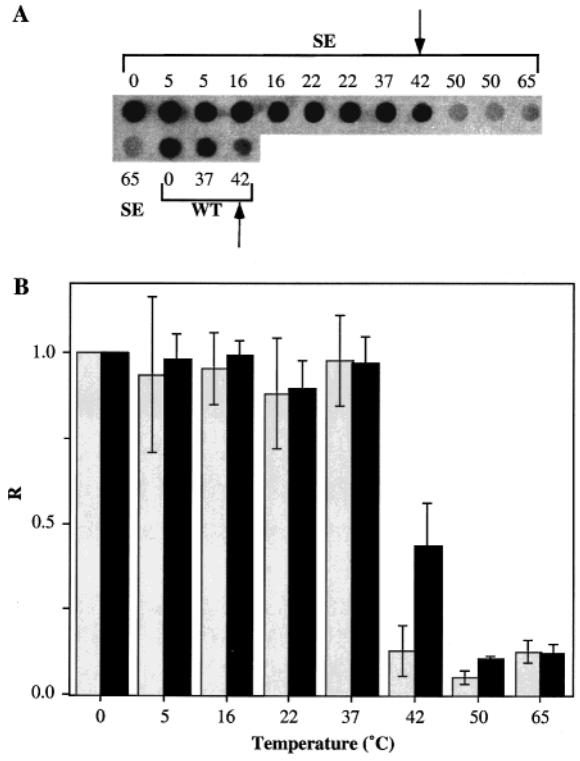

FIGURE 4: Ab1620 reactivity to wild-type and S392E proteins. (A) Representative film exposure for a conformational antibody experiment. After incubation at 0, 5, 16, 22, 37, 42, and 50 °C, samples of wild-type and S392E protein were filtered onto nitrocellulose and probed with p53 monoclonal antibody Ab1620. For the *representative* experiment shown, duplicate samples of S392E protein were filtered at each temperature with the exception of 0, 37, and 42 °C. Single samples of wild-type protein were filtered for 0, 37, and 42 °C for direct comparison to S392E behavior. Significant differences between the mutant and wild-type proteins could only be detected at 42 °C (arrows). (B) Results from multiple experiments that provided replicate samples ($n = 3$ to 5) at each temperature for each protein were quantitated by densitometry to yield reactivity data for wild-type (gray) and S392E (black) proteins. Reactivity at each temperature was measured relative to that of the specific protein at 0 °C for each experiment (defined as 1). Error bars indicate one standard deviation.

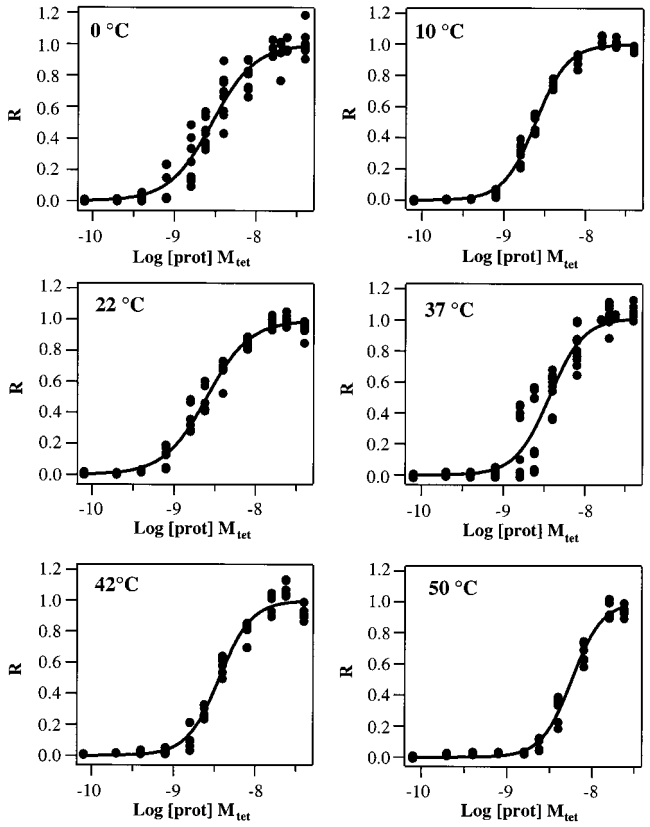

FIGURE 5: S392E−conDNA binding as a function of temperature. The concentration of conDNA was held constant at 2×10^{-11} M, and the concentration of S392E protein (reported as M tetramer) was varied as indicated. R describes the fractional saturation of protein−DNA complex. Experiments ($n = 3-5$) were conducted in duplicate. The solid line in each graph represents the fit of the data to eq 2. Temperature has only a minor effect on binding for S392E, with a 2-fold decrease observed in apparent dissociation constants (K_d) over the range investigated.

correlation between DNA binding and antibody reactivity. Experiments were conducted with the S392E protein to determine whether this antibody could detect the increased thermal stability of S392E apparent in CD experiments. Protein incubated at 0, 5, 16, 22, or 37 °C displayed Ab1620 reactivity levels undiminished from those observed at 0 °C, whereas incubation at 50 or 65 °C resulted in a substantial decrease in reactivity, similar to results for the wild-type protein (Figure 4). At 42 °C, however, reactivity to S392E was significantly greater than reactivity to the wild-type protein, further suggesting structural effects of the C-terminal substitution on the DNA binding domain of the mutant protein. Reaction to Ab421, which is sensitive to aggregation (Nichols, unpublished data) was unchanged with temperature for S392E over the entire temperature range examined, as observed for wild-type protein (*30*).

S392E ConDNA Binding. On the basis of previously published experiments (*19*−*22*, *26*−*28*), phosphorylation or mutation to an acid residue at the CKII site would be anticipated to result in an increased affinity for specific DNA binding. Previous studies reporting binding affinity enhancement for the phosphorylated or mutant proteins (*19*−*22*, *26*−*28*) utilized 20 bp DNA target sequences embedded in 25−26 bp oligonucleotides; however, no equilibrium dissociation constants have been reported for either S392E or wild-type p53 phosphorylated at this position. In light of results from experiments with wild-type protein that established the inhibitory nature of nonspecific DNA (*29*, *30*), present in previously published experiments, we examined S392E specific binding in the absence of these inhibitors. The double-stranded 20mer sequence, conDNA, was used to assay S392E specific binding by nitrocellulose filter binding (Figure 5). The apparent dissociation constant for S392E−conDNA at room temperature ($K_d = 2.5 \pm 0.2 \times 10^{-9}$ M_{tet}) was only slightly different from that reported previously for the wild-type protein ($K_d = 1.6 \pm 0.1 \times 10^{-9}$ M_{tet}) (*30*).

Thermal Insensitivity of S392E Specific DNA Binding. The DNA binding affinity of S392E for conDNA as a function of temperature was examined to determine whether increased structural stability would correlate with decreased thermal sensitivity for in vitro DNA binding. High affinity dsDNA binding by the S392E protein was measured from 0 to 50 °C (Figure 5, Table 1), and the observed dissociation constants varied only 2-fold over this temperature range. In contrast, wild-type DNA binding affinity for conDNA decreases ~5-fold over this temperature range (*30*).

Table 1: Observed Dissociation Constants (K_d) for S392E and Wild-Type p53 Sequence-Specific DNA Binding[a]

temp	S392E K_d (M_{tet})	WT[b] K_d (M_{tet})
0	$2.9 \pm 0.4 \times 10^{-9}$	$1.7 \pm 0.2 \times 10^{-9}$
10	$2.4 \pm 0.1 \times 10^{-9}$	$1.3 \pm 0.1 \times 10^{-9}$
22	$2.5 \pm 0.2 \times 10^{-9}$	$1.6 \pm 0.1 \times 10^{-9}$
37	$3.6 \pm 0.5 \times 10^{-9}$	$1.9 \pm 0.1 \times 10^{-9}$
42	$3.6 \pm 0.4 \times 10^{-9}$	$3.6 \pm 0.2 \times 10^{-9}$
50	$5.8 \pm 0.1 \times 10^{-9}$	$7.2 \pm 1.1 \times 10^{-9}$

[a] Dissociation constants (K_d) are derived from 3 to 6 experiments, performed in duplicate, and are corrected for protein activity. Binding was examined using the double-stranded 20mer base pair target sequence, conDNA. [b] From Nichols and Matthews (*30*).

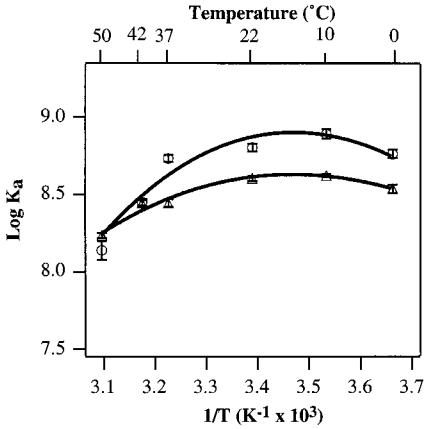

FIGURE 6: van't Hoff analysis of S392E DNA binding. The log of the association constants ($K_a = 1/K_d$) derived from conDNA binding experiments is plotted as a function of inverse temperature in degrees Kelvin to determine the heat capacity change upon conDNA binding to wild-type p53 (○) and S392E (△). The more concave the curvature of the fit (solid line), the greater the negative change in the heat capacity upon binding. Error bars indicate one standard deviation. Temperature in degrees Celsius is shown on the top axis for reference.

Thermodynamic analysis of S392E−conDNA binding, conducted as reported previously for the wild-type protein (*30*), revealed a decreased heat capacity change over the temperature range investigated (Figure 6). The ΔC_p for S392E specific DNA binding is estimated to be approximately half the already diminutive wild-type value (S392E, ~ -0.28 kcal/mol·K; WT, ~ -0.50 kcal/mol·K) (*30*). The lower negative heat capacity change in the mutant suggests that the binding interaction is devoid of significant conformational changes in either DNA or protein that bury apolar surfaces or restrict the motional freedom of the binding surfaces (*38*, *39*). This difference may derive from the increased structural stability of the S392E mutant protein.

Effect of Flanking Nonspecific DNA on DNA Binding of S392E and Wild-Type p53. A double-stranded 40 bp target DNA sequence (40DNA) was constructed to contain conDNA as its central 20 bases with 10 base pairs of flanking nonspecific sequence at both the 3′ and 5′ ends (Figure 1B). A 60 base pair DNA target was constructed by the addition of 20 base pairs of nonspecific sequence (NS2) onto the 5′ end of 40DNA (Figure 1B). These DNAs were designed to more closely represent sequences encountered in vivo and to determine whether flanking nonspecific sequences influenced specific DNA binding by either the S392E or the wild-type protein. DNA binding assays (Figure 7) revealed, if any change, a slight increase in S392E apparent affinity for 40DNA over the 20mer conDNA (Table 2). Wild-type 40DNA binding affinity, however, appeared to be slightly decreased as compared to that measured for conDNA. Binding to the double-stranded 60 base pair DNA target revealed a more significant 3-fold difference between the affinities of the two proteins, demonstrating a negative effect of flanking nonspecific DNA on the specific DNA binding function of wild-type, but not mutant, p53.

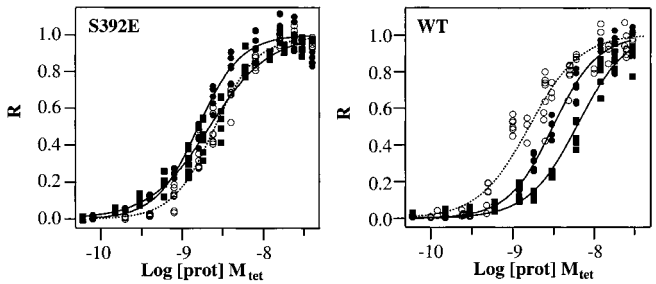

FIGURE 7: Binding of wild-type and S392E proteins to 20, 40, and 60 base pair target DNAs. 40DNA and 60DNA binding experiments were conducted as described for conDNA experiments. Data for 40DNA (●) and 60DNA (■) are the results of three experiments conducted in duplicate and were fit (solid lines) to eq 2. Dashed lines and open circles represent fitted curves and data points from conDNA experiments for reference.

Table 2: Observed Dissociation Constants (K_d) for S392E and Wild-Type p53 Sequence-Specific DNA Binding as a Function of DNA Target Length[a]

DNA	S392E K_d (M_{tet})	WT K_d (M_{tet})
conDNA	$2.5 \pm 0.2 \times 10^{-9}$	$1.6 \pm 0.1 \times 10^{-9}$
40DNA	$1.6 \pm 0.1 \times 10^{-9}$	$2.5 \pm 0.1 \times 10^{-9}$
60DNA	$2.1 \pm 0.2 \times 10^{-9}$	$6.6 \pm 0.7 \times 10^{-9}$

[a] Dissociation constants are derived from 3 to 6 experiments, performed in duplicate, and corrected for protein activity. Binding was examined using double-stranded 20, 40, or 60 base pair target sequences, conDNA, 40DNA, or 60DNA, each of which contain one copy of the p53 consensus sequence.

S392E Nonspecific DNA Binding. To determine whether increased binding to nonspecific DNA contributes to S392E maintaining high affinity binding to DNA targets containing flanking nonspecific sequence, affinity for the 20 bp nonspecific DNA sequence, NS2, was measured at 0, 22, and 50 °C. The apparent dissociation constant for S392E−NS2 binding was 1×10^{-8} M_{tet} and did not vary significantly over the temperature range investigated (Figure 8, Table 3). We have previously demonstrated that wild-type affinity for the same sequence was sufficiently low that it was not possible to generate complete binding curves (*30*). An estimate of the K_d for wild-type−NS2 interaction at 22 °C indicated a value $\sim 5 \times 10^{-8}$ M_{tet} corresponding to a significantly lower affinity than that for the mutant. More striking is that the S392E−NS2 affinity is only 2-fold lower than that for S392E−conDNA at 50 °C. Thus, the difference between specific and nonspecific binding is substantially decreased for this mutant protein as compared to wild-type p53. Addition of NS2 DNA inhibits S392E binding to conDNA slightly less than that observed for wild-type p53 (*30*), and this inhibition is reversed by Ab421 addition (data not shown).

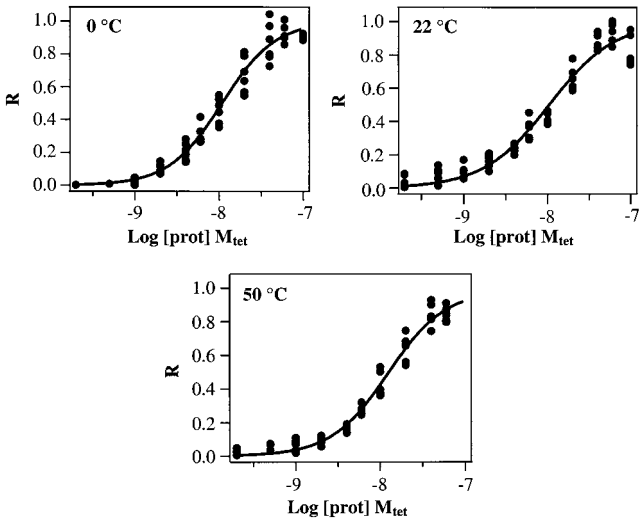

FIGURE 8: S392E nonspecific DNA binding as a function of temperature. Isotherms are shown for DNA binding experiments conducted at 0, 22, and 50 °C with the nonspecific double-stranded 20 base pair sequence, NS2, and purified S392E protein. *R* is the fraction of bound complex and is reported as a function of tetrameric protein concentration. The affinity of the protein for this target sequence (apparent $K_d \cong 1 \times 10^{-8}$ M_{tet}) does not vary significantly over this temperature range. Data points are the results of three experiments conducted in duplicate and were fit (solid line) to eq 2.

Table 3: Observed Dissociation Constants (K_d) for S392E and Wild-Type p53 Nonspecific DNA Binding[a]

temp	S392E $K_d \times 10^9$	WT $K_d \times 10^9$
0	11 ± 1	ND[b]
22	10 ± 2	~50[c]
50	12 ± 1	~100[c]

[a] Dissociation constants are derived from 3 to 6 experiments, performed in duplicate, and corrected for protein activity. Binding was examined using double-stranded 20mer base pair target sequence, NS2. [b] ND, not determined. [c] The absence of a saturation plateau for wild-type−NS2 experiments as reported previously (*30*) precludes a more rigorous analysis of this interaction.

DISCUSSION

p53 exhibits a low level of function—observed as lack of apoptosis and cell cycle arrest—in normal, undamaged cells; yet this protein can be activated to promote both these processes upon DNA damage and cellular stress (reviewed in ref *40*). Because of the high percentage of human cancer cells with nonfunctional p53 protein, identifying the mechanisms that generate p53 activation is of significant value (*13*, *14*, *41*−*43*). A myriad of cellular effects have been associated with DNA damage leading to p53 activation, including differential MDM2-mediated degradation of p53 and multiple p53 posttranslational modifications that affect function (reviewed in refs *16* and *44*).

Numerous DNA binding experiments have demonstrated the ability of the C-terminus of p53 to regulate sequence-specific DNA binding of the core domain in cell extracts or in the presence of nonspecific DNA. Deletion of the last 30 amino acids, incubation with antibody to the C-terminus (Ab421) or C-terminal peptides, as well as acetylation and serine 392 phosphorylation at the C-terminus have all been shown to enhance p53 DNA binding in the presence of nonspecific dsDNA (*19*−*22*, *26*−*29*, *45*−*47*). Mutation of serine 392 to glutamate (S392E) (*19*) has been deduced to mimic phosphorylation which increases activity of the modified protein both in vivo and in vitro in assays containing nonspecific DNA (*20*−*22*, *26*−*28*). However, the presence of nonspecific DNA has been demonstrated to inhibit sequence-specific DNA binding by the core domain (*29*, *30*, *48*), confusing the role of the C-terminus in p53 function. Further, understanding the role of the C-terminus is complicated by its own ability to bind nonspecific DNA (*49*). We have demonstrated the ability of bacterially produced wild-type "latent" p53 protein to bind specific DNA with high affinity in the absence of nonspecific DNA used prevalently in other assays (*30*). Introducing the S392E mutation into human p53 protein for bacterial expression allows exploration of the effects of an "activating" mutation on both the structure and function of p53 without the complication of other posttranslational modifications.

S392E protein structure, as monitored by circular dichroism spectroscopy, is significantly more stable than wild-type p53 structure. This enhanced stability is seen in the signals that reflect both β-sheet and α-helical structures, with minimal loss of β-sheet signal to temperatures as high as 100 °C. The slightly increased aggregation observed for S392E protein as compared to wild-type p53 might be considered a source of this difference. However, a similar enhancement in thermal stability is observed with deletion of the C-terminal 33 amino acids, and this Δ33 p53 exhibits no apparent aggregation beyond tetramer (Moraitis and Matthews, manuscript in preparation). As demonstrated previously, X-ray crystallographic and NMR structural data in concert with structure prediction algorithms indicate that the β-sheet CD signal corresponds almost exclusively to the core domain of p53 (*30*). Thus, a serine to glutamate mutation at the penultimate residue of the protein, well removed in sequence space from the core DNA binding domain, appears capable of exerting substantial effects on core domain structure. Whether the wild-type C-terminus destabilizes the core domain or the S392E C-terminus stabilizes this region cannot be discerned from these experiments, nor can we deduce whether direct interaction or conformational alterations at a distance mediate these effects.

Substitution of the serine modified by CKII with glutamic acid also appears to increase the content and thermal stability of α-helical structure in p53. Regions of p53 predicted to contain α-helical structure include the N- and C-termini, encompassing the tetramerization domain, as well as small portions of the core domain (*30*), precluding the identification of the specific region affected. Structures of peptides from wild-type p53 have indicated that segments of both the N- and C-termini are capable of forming helical structure in the presence of other protein domains (*50*, *51*), and effects of "activating" p53, mimicked by the S392E substitution, may stabilize such structures. The tetramerization domain is a four α-helical structure, and phosphorylation in the C-terminus also might stabilize assembly of this region, as observed for isolated peptide sequences (*52*). The observed tendency of S392E to form higher order (i.e., greater than tetramer) oligomeric structures also may be elicited by alterations associated with the negative charge introduced at position 392. Further studies will be necessary to determine the mechanisms of S392E stabilization of α-helical segments.

Increased thermal stability for the S392E protein was also observed using the monoclonal conformational antibody, Ab1620. Although reactivity with Ab1620 has been used previously to predict the presence or absence of DNA binding function, we have demonstrated that Ab1620 reactivity does not correlate directly with this function, particularly at high temperatures (*30*). However, the antibody may detect small conformational changes in the wild-type DNA binding core domain that are associated with the small decrease in DNA affinity observed between 37 and 42 °C (*30*). For the S392E protein, a decrease in Ab1620 reactivity is also observed in the same temperature range; however, the magnitude of decrease at 42 °C is diminished as compared to that measured for wild-type p53. Thus, increased structural stability of S392E detected by circular dichroism is also reflected in Ab1620 reactivity at 42 °C. Such differences in the thermal stability of S392E as compared to wild-type p53 could influence a number of processes that in turn may contribute to the observed "activated" phenotype in vivo (*19*, *23*, *24*).

The increased thermal stability of S392E is mirrored by a decreased functional sensitivity to elevated temperature. Apparent DNA binding constants for consensus DNA sequences decrease only ~2-fold from 0 to 50 °C, as compared to a ~5-fold decrease measured for the wild-type protein (*30*). Strikingly, an increase in overall affinity for specific DNA is not observed for this "activated" mutant, with apparent equilibrium binding constants for S392E near or above wild-type levels at most temperatures. At 50 °C, however, S392E binding affinity for consensus DNA sequences surpasses wild-type p53 values. Interestingly, substantial structural differences become apparent for the wild-type protein at 50 °C, whereas the S392E β-sheet signal is not diminished to 100 °C. Since the β-sheet signal corresponds to the core DNA binding domain (*30*), enhanced stability in this region may account for the ability of the S392E protein to maintain DNA affinity at elevated temperatures. The absence of a large negative ΔC_p for p53−conDNA binding suggested a rigid structure that provides a unique lock-and-key binding surface with minimal conformational alteration upon DNA binding (*30*). The ~2-fold lower ΔC_p for S392E−conDNA binding as compared to the wild-type interaction suggests even less motional flexibility. The introduction of a negative charge at position 392 appears to enhance rigidity and thermal stability of the core domain. This view of p53 structure is supported by the comparison of recently published crystal structures of the free form of the murine p53 core domain (*53*) with the DNA bound human p53 core domain (*54*). The structure of the central core domain β-sheet sandwiches of these two forms of p53, even from different organisms, are identical, and significant spatial rearrangements are detected only in the small L1 loop (residues 115−121) that contacts the DNA (*53*).

Given the added negative charge of the glutamate side chain and presuming that the C-terminus is the primary site for nonspecific binding, the fact that the S392E mutant binds to nonspecific DNA with a greater affinity than the wild-type p53 protein is particularly noteworthy. Further, at elevated temperatures, nonspecific S392E binding affinities closely approach (~2-fold difference) those for S392E specific DNA binding. This result suggests a diminished ability of the mutant (and presumably "activated") protein to distinguish between p53 response elements (p53REs) and random nonspecific DNA and does not intuitively correlate with the concept of a "guardian of the genome" searching out p53REs to initiate apoptosis or cell cycle arrest when activated. Because phosphorylation or mutation at the CKII site reportedly leads to an activated p53 phenotype in vivo (*19*, *23*, *24*), some variation in function must exist between the wild-type and a protein modified at this site. Results from our investigation of longer target DNAs, containing both specific and nonspecific sequences to more closely represent DNAs encountered in vivo, provides one possible explanation. Wild-type affinity for targets containing the consensus sequence is decreased as the proportion of nonspecific DNA is increased, whereas S392E affinity remains unaltered for these sequences. This distinction generates a functional gap between the two proteins. Since increased nonspecific DNA binding activity can enhance S392E binding to specific DNA sequences embedded in nonspecific backgrounds, the "activated" protein may display increased affinity for p53REs in vivo even though affinity for the 20 bp consensus DNA is similar to wild-type p53 in vitro.

The discovery of significant differences between wild-type p53 and an "activated" mutant protein, including thermal stability and affinity for both nonspecific DNA and specific DNA sequences embedded in nonspecific DNAs, provides essential elements for understanding the differences between these states of p53 and discerning structural and functional effects of "activation." These observations lay the foundation for experiments that can address the regulation of both specific and nonspecific DNA binding and explore effects of additional physiologically relevant protein modifications and interactions.

ACKNOWLEDGMENT

We thank Emilia Mrowczynski for early development of the methods used in protein purification and Markos Moraitis for many helpful discussions.

REFERENCES

1. Maltzman, W., and Czyzyk, L. (1984) *Mol. Cell. Biol. 4*, 1689−1694.
2. Raycroft, L., Wu, H., and Lozano, G. (1990) *Science 249*, 1049−1051.
3. El-Deiry, W. S., Kern, S. E., Pietenpol, J. A., Kinzler, K. W., and Vogelstein, B. (1992) *Nat. Genet. 1*, 45−49.
4. Funk, W. D., Pak, D. T., Karas, R. H., Wright, W. E., and Shay, J. W. (1992) *Mol. Cell. Biol. 12*, 2866−2871.
5. Kastan, M. B., Zhan, Q., El-Deiry, W. S., Carrier, F., Jacks, T., Walsh, W. V., Plunkett, B. S., Vogelstein, B., and Fornace, A. J., Jr. (1992) *Cell 71*, 587−597.
6. Momand, J., Zambetti, G. P., Olson, D. C., George, D., and Levine, A. J. (1992) *Cell 69*, 1237−1245.
7. Foord, O., Navot, N., and Rotter, V. (1993) *Mol. Cell. Biol. 13*, 1378−1384.
8. El-Deiry, W. S. (1998) *Semin. Cancer Biol. 8*, 345−357.
9. Kern, S. E., Kinzler, K. W., Bruskin, A., Jarosz, D., Friedman, P., Prives, C., and Vogelstein, B. (1991) *Science 252*, 1708−1711.
10. Bargonetti, J., Friedman, P. N., Kern, S. E., Vogelstein, B., and Prives, C. (1991) *Cell 65*, 1083−1091.
11. Foord, O. S., Bhattacharya, P., Reich, Z., and Rotter, V. (1991) *Nucleic Acids Res. 19*, 5191−5198.
12. Bargonetti, J., Manfredi, J. J., Chen, X., Marshak, D. R., and Prives, C. (1993) *Genes Dev. 7*, 2565−2574.
13. Hernandez-Boussard, T., Rodriguez-Tome, P., Montesano, R., and Hainaut, P. (1999) *Hum. Mutat. 14*, 1−8.

14. Soussi, T., Dehouche, K., and Béroud, C. (2000) *Hum. Mutat. 15*, 105−113.
15. Meek, D. W. (1997) *Pathol. Biol. 45*, 804−814.
16. Appella, E., and Anderson, C. W. (2000) *Pathol. Biol. 48*, 227−245.
17. Meek, D. W., Simon, S., Kikkawa, U., and Eckhart, W. (1990) *EMBO J. 9*, 3253−3260.
18. Filhol, O., Baudier, J., Delphin, C., Loue-Mackenbach, P., Chambaz, E. M., and Cochet, C. (1992) *J. Biol. Chem. 267*, 20577−20583.
19. Hao, M., Lowy, A. M., Kapoor, M., Deffie, A., Liu, G., and Lozano, G. (1996) *J. Biol. Chem. 271*, 29380−29385.
20. Hupp, T. R., and Lane, D. P. (1995) *J. Biol. Chem. 270*, 18165−18174.
21. Hupp, T. R., and Lane, D. P. (1994) *Cold Spring Harbor Symp. Quant. Biol. 59*, 195−206.
22. Kapoor, M., Hamm, R., Yan, W., Taya, Y., and Lozano, G. (2000) *Oncogene 19*, 358−364.
23. Milne, D. M., Palmer, R. H., and Meek, D. W. (1992) *Nucleic Acids Res. 20*, 5565−5570.
24. Hall, S. R., Campbell, L. E., and Meek, D. W. (1996) *Nucleic Acids Res. 24*, 1119−1126.
25. Fiscella, M., Zambrano, N., Ullrich, S. J., Unger, T., Lin, D., Cho, B., Mercer, W. E., Anderson, C. W., and Appella, E. (1994) *Oncogene 9*, 3249−3257.
26. Hupp, T. R., Meek, D. W., Midgley, C. A., and Lane, D. P. (1992) *Cell 71*, 875−886.
27. Hupp, T. R., Meek, D. W., Midgley, C. A., and Lane, D. P. (1993) *Nucleic Acids Res. 21*, 3167−3174.
28. Hupp, T. R., and Lane, D. P. (1994) *Curr. Biol. 4*, 865−875.
29. Anderson, M. E., Woelker, B., Reed, M., Wang, P., and Tegtmeyer, P. (1997) *Mol. Cell. Biol. 17*, 6255−6264.
30. Nichols, N. M., and Matthews, K. S. (2001) *Biochemistry 40*, 3847−3858.
31. Kunkel, T. A. (1985) *Proc. Natl. Acad. Sci. U.S.A. 82*, 488−492.
32. Harlow, E., Crawford, L. V., Pim, D. C., and Williamson, N. M. (1981) *J. Virol. 39*, 861−869.
33. Gannon, J. V., Greaves, R., Iggo, R., and Lane, D. P. (1990) *EMBO J. 9*, 1595−1602.
34. Bradford, M. M. (1976) *Anal. Biochem. 72*, 248−254.
35. Wong, I., and Lohman, T. M. (1993) *Proc. Natl. Acad. Sci. U.S.A. 90*, 5428−5432.
36. Ha, J.-H., Spolar, R. S., and Record, M. T., Jr. (1989) *J. Mol. Biol. 209*, 801−816.
37. Hansen, S., Hupp, T. R., and Lane, D. P. (1996) *J. Biol. Chem. 271*, 3917−3924.
38. Spolar, R. S., and Record, M. T., Jr. (1994) *Science 263*, 777−784.
39. Ladbury, J. E., Wright, J. G., Sturtevant, J. M., and Sigler, P. B. (1994) *J. Mol. Biol. 238*, 669−681.
40. Levine, A. J. (1997) *Cell 88*, 323−331.
41. Mulligan, L. M., Matlashewski, G. J., Scrable, H. J., and Cavenee, W. K. (1990) *Proc. Natl. Acad. Sci. U.S.A. 87*, 5863−5867.
42. Moll, U. M., Riou, G., and Levine, A. J. (1992) *Proc. Natl. Acad. Sci. U.S.A. 89*, 7262−7266.
43. Moll, U. M., LaQuaglia, M., Bénard, J., and Riou, G. (1995) *Proc. Natl. Acad. Sci. U.S.A. 92*, 4407−4411.
44. Prives, C., and Hall, P. A. (1999) *J. Pathol. 187*, 112−126.
45. Hupp, T. R., Sparks, A., and Lane, D. P. (1995) *Cell 83*, 237−245.
46. Selivanova, G., Ryabchenko, L., Jansson, E., Iotsova, V., and Wiman, K. G. (1999) *Mol. Cell. Biol. 19*, 3395−3402.
47. Gu, W., and Roeder, R. G. (1997) *Cell 90*, 595−606.
48. Bayle, J. H., Elenbaas, B., and Levine, A. J. (1995) *Proc. Natl. Acad. Sci. U.S.A. 92*, 5729−5733.
49. Selivanova, G., Iotsova, V., Kiseleva, E., Ström, M., Bakalkin, G., Grafström, R. C., and Wiman, K. G. (1996) *Nucleic Acids Res. 24*, 3560−3567.
50. Kussie, P. H., Gorina, S., Marechal, V., Elenbaas, B., Moreau, J., Levine, A. J., and Pavletich, N. P. (1996) *Science 274*, 948−953.
51. Rustandi, R. R., Baldisseri, D. M., and Weber, D. J. (2000) *Nat. Struct. Biol. 7*, 570−574.
52. Sakaguchi, K., Sakamoto, H., Xie, D., Erickson, J. W., Lewis, M. S., Anderson, C. W., and Appella, E. (1997) *J. Prot. Chem. 16*, 553−556.
53. Zhao, K., Chai, X., Johnston, K., Clements, A., and Marmorstein, R. (2001) *J. Biol. Chem. 276*, 12120−12127.
54. Cho, Y., Gorina, S., Jeffrey, P. D., and Pavletich, N. P. (1994) *Science 265*, 346−355.

BI011736R